Biochimica et Biophysica Acta 1798 (2010) 1014–1019

Contents lists available at ScienceDirect

Biochimica et Biophysica Acta

journal homepage: www.elsevier.com/locate/bbamem

# Preferential insertion of lactose permease in phospholipid domains: AFM observations

Laura Picas [a], Adrián Carretero-Genevrier [d], M. Teresa Montero [a,b], J.L. Vázquez-Ibar [c], Bastien Seantier [e], Pierre-Emmanuel Milhiet [e,f], Jordi Hernández-Borrell [a,b,*]

[a] Departament de Fisicoquímica, Facultat de Farmàcia, Universitat de Barcelona (UB), Spain
[b] Institut de Nanociència i Nanotecnologia de la Universitat de Barcelona (IN2UB), Spain
[c] ICREA and Institut de Recerca Biomèdica, Parc Científic de Barcelona, 08028 Barcelona, Spain
[d] Institut de Ciencia de Materials de Barcelona ICMAB, Consejo Superior de Investigaciones Científicas (CSIC), 08193 Bellaterra, Spain
[e] Inserm, Unité 554, Montpellier, France
[f] Université de Montpellier, CNRS, UMR 5048, Centre de Biochimie Structurale, Montpellier, France

ARTICLE INFO

*Article history:*
Received 18 November 2009
Received in revised form 1 January 2010
Accepted 11 January 2010
Available online 21 January 2010

*Keywords:*
Lactose permease
AFM
Phospholipid domains

ABSTRACT

We report the insertion of a transmembrane protein, lactose permease (LacY) from *Escherichia coli* (*E. coli*), in supported lipid bilayers (SLBs) of 1-palmitoyl-2-oleoyl-*sn*-glycero-3-phosphoethanolamine (POPE) and 1-palmitoyl-2-oleoyl-*sn*-glycero-3-phosphoglycerol (POPG), in biomimetic molar proportions. We provide evidence of the preferential insertion of LacY in the fluid domains. Analysis of the self-assembled protein arrangements showed that LacY: (i) is inserted as a monomer within fluid domains of SLBs of POPE:POPG (3:1, mol/mol), (ii) has a diameter of approx. 7.8 nm; and (iii) keeps an area of phospholipids surrounding the protein that is compatible with shells of phospholipids.



## 1. Introduction

Membrane proteins account for over 25% of total cell proteins. The cytoplasmic membrane of *Escherichia coli*, for instance, is believed to contain more than 200 protein types, of which 60 or more may be involved in transport functions. Among them, lactose permease (LacY), one of the most exhaustively studied cytoplasmic membrane proteins, is often taken as a paradigm for secondary transport proteins that couple the energy stored in an electrochemical ion gradient to a concentration gradient (β-galactoside/$H^+$ symport). LacY belongs to the Major Facilitator Superfamily (MFS), (http://www.tcdb.org/), a large group of membrane transport proteins that are evolutionarily related. LacY consists of twelve transmembrane α-helices, crossing the membrane in a zig-zag fashion, that are connected by eleven relatively hydrophilic, periplasmic and cytoplasmic loops, with both amino and carboxyl termini on the cytoplasmic surface. Before LacY's crystallization, site-directed mutagenesis in combination with biochemical and biophysical studies provided indirect information on its tertiary structure [1,2]. However, repeated failures to obtain three-dimensional (3D) crystals, even using fusion proteins containing soluble domains inserted into various loops of LacY [3,4], remained a basic limitation in determining any precise structural information on the mechanisms underlying protein activity. It was not until 3D crystals from a mutant of LacY, with Gly in place of Cys154 (C154G), were obtained of sufficient quality for high-resolution X-ray diffraction studies that a plausible mechanism for lactose/proton symport was suggested [5]. More recently, it has been shown that LacY crystallizes differently in different systems, depending on the amount of phospholipid present [2]. In addition, two-dimensional crystallization of LacY has been achieved in the presence of zwitterionic phospholipids [6,7].

Difficulties encountered in LacY crystallization reflect the difficulties of maintaining the purified protein in a favourable physicochemical environment. LacY is an extremely hydrophobic and flexible protein [8–10] that, after extraction from *E. coli* membranes, is obtained in detergents of low cmc and may often undergo self-aggregation because of its high hydrophobicity. Nevertheless, the protein can easily be reconstituted into proteoliposomes by conventional procedures [11]. Thus, for instance, LacY has been reconstituted in native *E. coli* polar phospholipid membrane extracts [12,13], in neutral phosphatidylcholine (PC) matrices [14] and in binary mixtures of phosphatidylglycerol (PG) and phosphatidylethanolamine (PE) [8,15,16]. PG and PE are normally selected because they widely mimic the phospholipid composition of *E. coli*.

In this study we used Atomic Force Microscopy (AFM) to investigate the insertion of LacY in Supported Lipid Bilayers (SLBs) of POPE:POPG (3:1, mol/mol). To reconstitute LacY into SLBs, we used a

* Corresponding author. Departament de Fisicoquímica, Facultat de Farmàcia, Av. Diagonal s.n. 08028-Barcelona, Spain.
*E-mail address:* jordihernandezborrell@ub.edu (J. Hernández-Borrell).

0005-2736/$ – see front matter © 2010 Elsevier B.V. All rights reserved.
doi:10.1016/j.bbamem.2010.01.008

method that basically consists of direct incorporation of the solubilized protein into SLBs previously destabilized with detergent [17].The specific objectives of this paper were to investigate: (i) whether the insertion method is applicable to LacY as a representative of secondary active transport proteins; and (ii) the distribution of LacY in the SLBs constituted by POPE:POPG (3:1, mol/mol).

## 2. Materials and methods

1-Palmitoyl-2-oleoyl-*sn*-glycero-3-phosphoethanolamine (POPE), specified as 99% pure, and 1-palmitoyl-2-oleoyl-*sn*-glycero-3-phosphoglycerol (POPG) were purchased from Avanti Polar Lipids (Alabaster, AL, USA). Buffer A consisted of 20 mM Hepes (pH 7.40) 150 mM NaCl; buffer B, of 20 mM Hepes (pH 7.40) 150 mM NaCl, 10 mM $CaCl_2$; and buffer C, of 20 mM Hepes (pH 7.40) 150 mM NaCl, 20 mM $CaCl_2$. All buffers were prepared in Ultrapure water (Milli Q® reverse osmosis system, 18.3 MΩ·cm resistivity). HPLC-grade chloroform and methanol and n-dodecyl β-D-maltoside (DDM) were purchased from SIGMA (St. Louis, MO, USA).

### 2.1. Bacterial strains and protein purification

Plasmid pCS19 encoding single-W151/C154G LacY with a 6-His tag at the C terminus was generated as described [18]. It was provided by Dr. H. Ronald Kaback (UCLA, USA). *E. coli* BL21(DE3) cells (Novagen, Madison, WI, USA) transformed with this plasmid were grown in 6.4 L of Luria–Bertani broth at 30 °C containing ampicillin (100 μg/ml) to an absorbance (600 nm) of 0.6 and induced with 0.5 mM isopropyl 1-thio-β-D-galactopyranoside. Cells were disrupted by passage through a French pressure cell, and the membrane fraction was harvested by ultracentrifugation. Membranes were solubilized by adding DDM to a final concentration of 2%, and LacY was purified by Co (II) affinity chromatography (Talon Superflow™, Palo Alto, CA, USA). Protein eluted with 150 mM imidazole was dialyzed against 20 mM Tris–HCl (pH 7.5), 0.008% DDM, concentrated by using Vivaspin 20 concentrators (30 kDa cutoff; Vivascience, Germany) and stored on ice. As determined by sodium dodecylsulfate/12% polyacrylamide gel electrophoresis followed by Coomassie blue staining, a single band with an apparent molecular weight of 36 kDa was observed. Protein concentration was assayed by using a micro-BCA kit (Pierce, Rockford, IL).

### 2.2. SLB formation and LacY reconstitution

SLBs were prepared according to a method described elsewhere [17]. Briefly, large unilamellar vesicles (LUVs) were prepared by extrusion of MLVs of POPE:POPG (3:1, mol:mol) in buffer A through 100 nm pore filters (Nucleopore). LUVs were deposited onto freshly cleaved mica disks mounted on a Teflon o-ring and incubated at 50 °C for 2 h in an oven. Bilayers were always kept in an aqueous environment and carefully rinsed before imaging with the same buffer. Before protein incorporation, presence of calcium on the SLBs was removed by exchanging buffer A with C. The sample was incubated with buffer C for 10 min and afterwards cleaned with buffer B for 45 min. Protein was incorporated by incubating SLBs in buffer B for 30 min at 4 °C with a 50 μl drop of buffer supplemented with DDM below the cmc (cmc/2), followed by 15 min incubation at 4 °C with the detergent at twice the cmc in presence of solubilized LacY at 20 μg/ml. The same procedure was done without protein to obtain a reference sample. Finally, detergent was removed by extensive washing of the samples with free-detergent buffer.

### 2.3. AFM imaging

AFM experiments were performed with a multimode microscope controlled by Nanoscope IIIa electronics (Veeco Instruments Inc., Santa Barbara, CA). Images were acquired in tapping mode (TM-AFM) at minimum vertical force, maximized amplitude setpoint value and with vibration amplitude kept as low as possible. V-shaped $Si_3N_4$ cantilevers (MSCT-AUNM, Veeco, CA) with a nominal spring constant of 0.10 N $m^{-1}$ were used in liquid operation.

### 2.4. Image processing

Image processing was done by using Gwyddion software (http://gwyddion.net), which is a modular program for SPM (scanning probe microscopy), for data visualization and analysis. When the discrete nature of the AFM scans contain $N \times N$ equidistant pixels, the two-dimensional (2D) height–height correlation function can be defined as $C(r) = \langle [z(r_0 + r) - \langle z \rangle][z(r_0) - \langle z \rangle] \rangle$, where $\langle ... \rangle$ means the average over all possible pairs in the matrix that are separated by a vector $r = xe_x + ye_y$. The $z$ values that are taken into account in the Eq. are the deviation from the average height $\langle z \rangle$ [19].

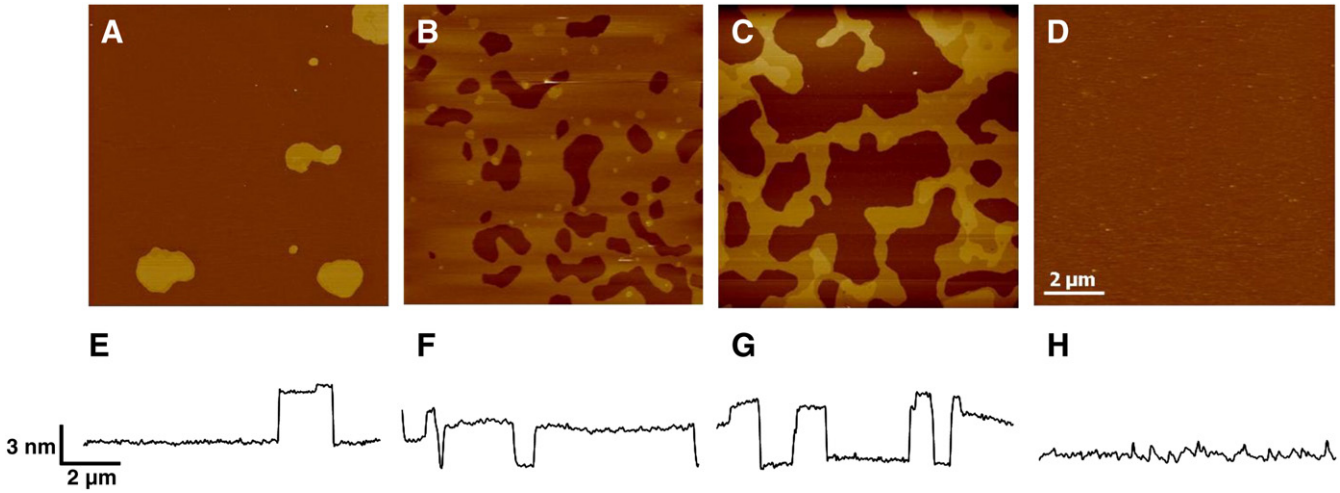


**Fig. 1.** Tapping® mode AFM images showing DDM effect on SLBs of POPE:POPG (3:1, mol/mol). Panel A shows topography of such SLBs after vesicle fusion performed in 20 mM Hepes, 150 mM NaCl, 10 mM $CaCl_2$ (pH 7.40) (A) buffer. Once the calcium was removed from SLBs (see Materials and methods), samples were incubated with DDM at the cmc (B), 2cmc (C) and 5cmc (D), at 4 °C. A cross-section taken along the white-dashed line on the topographic images is shown beneath the topographic images (E, F, G, and H, respectively). The $z$-colour scale is 25 nm and the scale bar is 2 μm.

**Table 1**
Mean value of the step-height differences between the substrate and both liquid-crystalline ($L_\alpha$) and gel ($L_\beta$) phase obtained from line profile analysis performed on Fig. 1E, F, G and H before (0 mM) and after addition of DDM at cmc, 2cmc and 5cmc, respectively.

| Fig. 1 | Height ($h$) (nm) | | |
|---|---|---|---|
| | DDM concentration (4 °C) | $\Delta h$ $L_\alpha$ | $\Delta h$ $L_\beta$ |
| E | 0 mM | – | 3.79 ± 0.19 |
| F | cmc | 4.24 ± 0.13 | 5.81 ± 0.22 |
| G | 2cmc | 4.30 ± 0.18 | 5.53 ± 0.28 |
| H | 5cmc | – | – |

**Table 2**
Mean value of the step-height differences between the substrate and the liquid-crystalline ($L_\alpha$) and gel ($L_\beta$) phases and protein-assembled patches obtained from cross-section analysis carried out on Figs. 2B, C, 5B and 5C.

| Figure | Height ($h$) (nm) | | |
|---|---|---|---|
| | $\Delta h$ $L_\alpha$ | $\Delta h$ $L_\beta$ | $\Delta h$ protein patches |
| 2B | 4.29 ± 0.10 | 5.50 ± 0.73 | |
| 2C | 4.21 ± 0.09 | – | 6.26 ± 0.12 |
| 5B | 4.30 ± 0.34 | 5.54 ± 0.26 | – |
| 5C | – | – | 6.22 ± 0.24 |

## 3. Results and discussion

The strategy for the reconstitution of transmembrane proteins into SLBs [17] consists of a four-step process: (i) formation of the SLBs; (ii) destabilization of the SLBs with detergent; (iii) addition of the solubilized protein in detergent; and (iv) removing detergent by extensive washing. In this method, the critical point is to find the optimal concentration of detergent for the destabilization of the bilayer that will eventually allow protein insertion. This concentration may differ, depending on the phospholipid composition of the SLB and from one protein to another [20]. Therefore, before any attempt for LacY insertion, we have monitored the effect of DDM on SLBs of POPE:POPG (3:1, mol:mol). SLBs obtained after deposition of liposomes onto mica are shown in Fig. 1A. As previously reported [21], two domains can be observed. Cross-sectional analysis (Fig. 1E) at the line drawn in the topographic image (Fig. 1A) makes clear the height difference between the two phospholipid phases. Actually, from the AFM topographic images we cannot infer the fluid or gel-like nature of each phospholipid domain. However, previous force spectroscopy measurements of SLBs of POPE:POPG [21] showed that the break-through force (the force that the bilayer can withstand without breaking) was 0.24 nN and 0.9 nN for the lower and upper domain, respectively. Therefore, these values were assigned to the liquid-crystalline ($L_\alpha$) and gel ($L_\beta$) phases, respectively. However, the step-height difference between the two phases was 3.79 ± 0.18 nm ($n = 10$) (see Table 1). This value, larger than expected but previously reported in other phase-separated SLBs [22], can be explained by repulsion between the tip and negatively charged POPG polar head, resulting in an overestimation of the height [20].

After addition of DDM at its cmc (Fig. 1B), incubated for 15 min at 4 °C (membranes are first destabilized for 30 min at 4 °C with DDM at the cmc/2) and washing with detergent-free buffer, the SLBs become partially solubilized, resulting in areas of uncovered mica. Larger uncovered areas appear for the highest concentration of DDM used (2cmc) (Fig. 1C). Regardless of the DDM concentration, in both topographic images, height differences between $L_\alpha$ and $L_\beta$ phases were lower than the height observed before DDM incubation (Table 1). Possibly, the introduction of DDM induces changes in the composition of each domain, which result in a decrease in the step-height difference between $L_\alpha$ and $L_\beta$ phases. The difference between the two phases (see the cross-section analysis in Fig. 1F and G) corroborates other differences found in the literature for $L_\alpha$ and $L_\beta$ phases [22]. Upon addition of DDM at 5cmc, the SLB is completely removed (Fig. 1D), as demonstrated by the cross-section profile (Fig. 1H).

The incorporation of membrane proteins into phospholipid matrices leads to self-assembled structures [23]. Fig. 2A shows another SLB of POPE:POPG (3:1, mol/mol) after being destabilized by DDM at 2cmc and washed with free-DDM buffer. The features are similar to those observed in Fig. 1B and C and laterally segregated domains, $L_\alpha$ and $L_\beta$ phases, are clearly observed. After 15 min incubation with 20 μg mL$^{-1}$ of LacY solubilized in DDM following

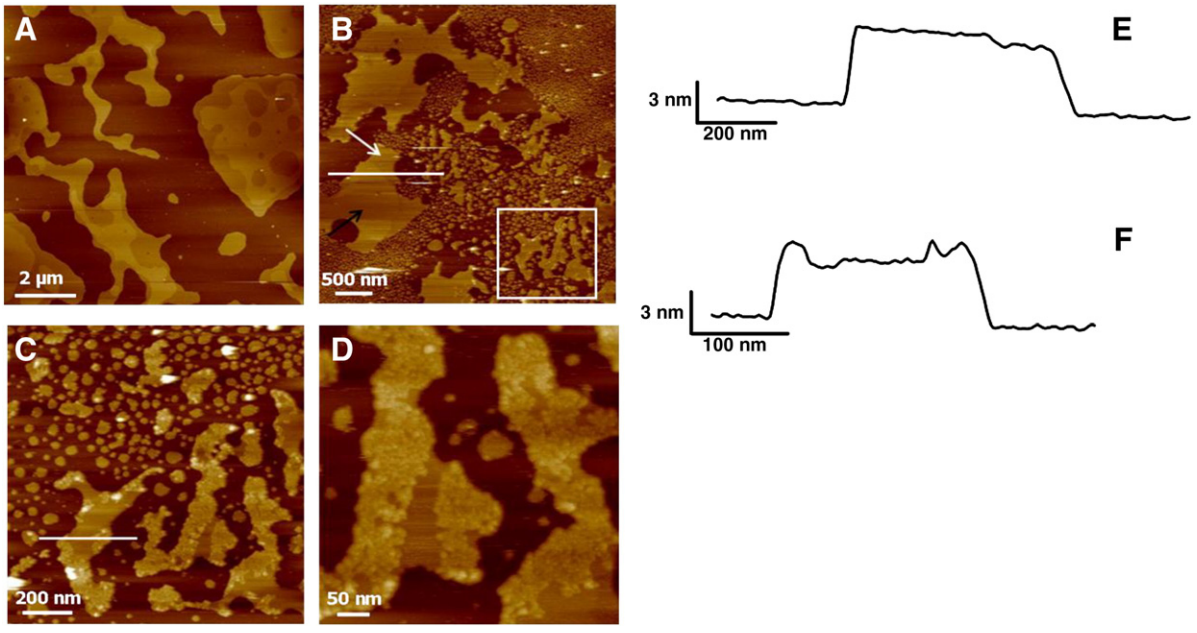


**Fig. 2.** TM-AFM images showing the topography of SLBs of POPE:POPG (3:1, mol/mol) after performing protein incorporation procedure (see Materials and methods) in absence (A) and in presence (B) of 20 μg/ml of LacY, respectively. Progressive magnifications on the highlighted area (white square) in panel A are shown in panels C and D, respectively. The $z$-colour scale is 25 nm and the scale bar is 2 μm, 500 nm, 200 nm and 50 nm for panels A, B, C and D, respectively.

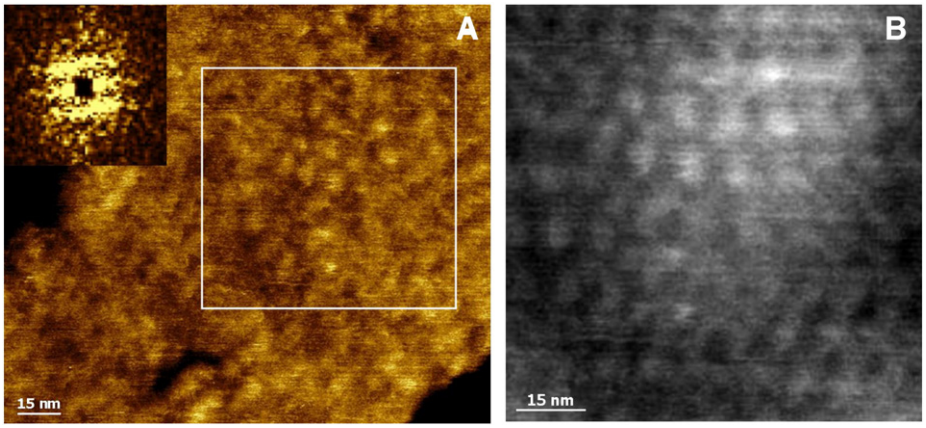


**Fig. 3.** Higher magnification TM-AFM image of the close-packed assemblies of protein presented in Fig. 2C and D (A). Inset 2D FFT of the topographic image, showing the distance between individual proteins. The *z*-colour scale is 7 nm and the scale bar is 15 nm. Inverse Fourier transform obtained from 2D FFT filtered image of the highlighted area in panel A is shown in panel B, showing repetitive round-shaped entities that correspond to individual monomeric proteins.

detergent removal, patches with different size and morphology are observed (Fig. 2B). Whilst there are patches showing both $L_\alpha$ (white arrow) and $L_\beta$ (black arrow) phases, that accordingly to the cross-section analysis (Fig. 2E) performed at the line drawn in Fig. 2B show a step-height difference of 1.21 nm (Table 2), other areas show higher corrugation (white square). Medium magnification of this latter area (Fig. 2C) revealed the presence of close-packed assemblies protruding above the $L_\alpha$ phase. This can be better appreciated following the line profile analysis at the line drawn in Fig. 2C which is provided in Fig. 2F. There, it can be seen that the close-packed assemblies reside in a domain with a height (4.21 nm) that coincides with the one observed for the $L_\alpha$ phase (see Table 2). By imaging the same region at a higher magnification (Fig. 2D) features of an internal structure are showed. Because these structures were not observed in absence of protein (Fig. 2A), these entities should most probably be attributed to protein molecules.

On closer inspection of protein-packed areas, the existence of a certain ordered arrangement is suggested (Fig. 3). However, the AFM image itself does not provide any clue concerning a possible symmetry. Besides, because of its flexibility, the probability of obtaining a defined crystalline packing is very low. Then, after applying a mask to minimize the noise in the two-dimensional Fast Fourier Transform (2D-FFT) (Fig. 3A, inset) we can observe in the inverse Fourier transform image (Fig. 3B) what it could be a local closed package of proteins with a defined nearest-neighbour separation. Individual entities, most probably protein monomers, surrounded by putative annular regions constituted of phospholipids, might be distinguished. From these results, it is difficult to assign any particular arrangement. More, having into account the extreme flexibility of the protein and its ability to get crystallised in several systems depending on the conditions and on the lipid protein ratio [2,6,7]. As discussed elsewhere, the hydrophobic surface of membrane proteins is covered by a shell of phospholipids known as boundary or annular phospholipids [24]. In this regard, by using Förster Resonance Energy Transfer (FRET) tools, we have shown that the annular region of LacY is slightly enriched in POPE, but that POPG is also present [16]. On the other hand, the separation between two entities can be estimated from the 2D-FFT (Fig. 3A, inset). Thus, the high-intensity lines shown in the 2D-FFT indicate a long-range ordering of proteins with a distance between them being $1/d = 12$ nm. To get further insight on the structural arrangement of the proteins, the normalized surface autocorrelation function corresponding to the topological AFM image shown in Fig. 3A was calculated (Fig. 4A). A skewed pattern of lines appears, indicating that proteins are, somehow, regularly arranged. Fig. 4B shows the profiles of the autocorrelation function, where 9 intense peaks can be observed in a perpendicular direction. Non-vanishing oscillations at large distances indicate long-range order in the protein network, as already detected by the 2D-FFT. Along protein lines, the first maximum is observed by describing the

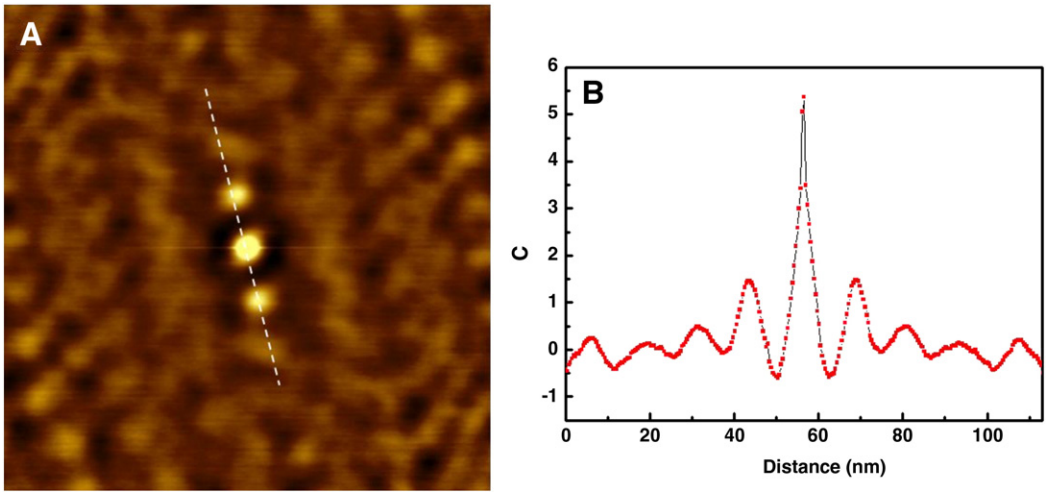


**Fig. 4.** Autocorrelation function of the topographic image shown in Fig. 3A (A) with the corresponding profile (B) along the white-dashed lines, indicating the length between each repetitive element found in the image against C, which is the value of the height–height correlation function.

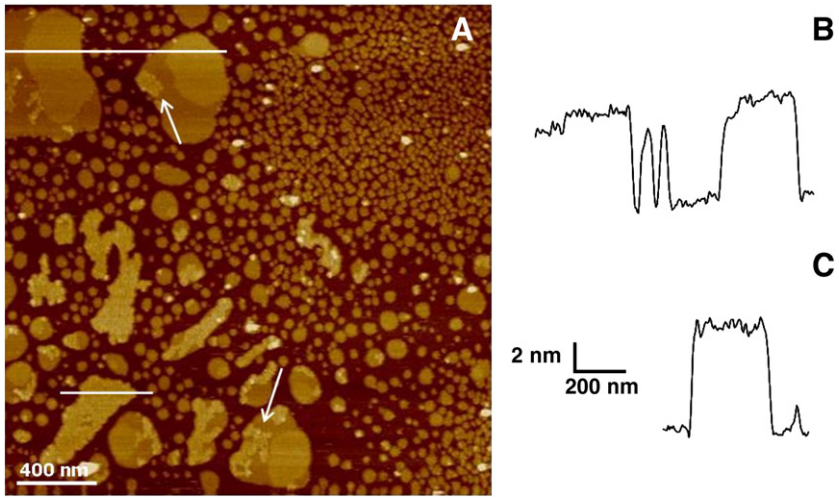


**Fig. 5.** TM-AFM image of an SLB of POPE:POPG (3:1, mol/mol) after protein incorporation with 20 μg/ml of LacY (A). White arrows point to the presence of close-packed assemblies of protein in one of the two lipid phases present in the sample. Cross-section analysis along white lines in the upper and lower left side of the image is shown in panels 5B and C, respectively. The *z*-colour scale is 15 nm and the scale bar is 400 nm.

nearest-neighbour separation distance. The average distances determined between two maxima of the repetitive elements in the autocorrelation functions is = 12.0 nm. Therefore, if the diameter of each round-shaped entity is $d = 7.8 \pm 1.0$ nm ($n = 15$) (Fig. 3A), we can assume that the persistence length between two proteins, i.e. the range over which different proteins can "feel" each other through the lipid bilayer [25], is $4.2 \pm 1.0$ nm. Then, assuming an average diameter of 0.7 nm for phospholipid molecules [26], each LacY protein would be surrounded by a microdomain consisting of three annular lipid shells [16]. This small (nanometer)-scale organization around LacY has been attributed to the hydrophobic-matching principle [27] and, as mentioned above, should be formed by annular phospholipids in fluid phase in order to provide adequate adaptation to the protein surfaces during the conformational changes that take place during transport [28].

Fig. 5A shows large patches that show both $L_\alpha$ and $L_\beta$ phases. The cross-section analysis (Fig. 5B) at the line drawn on top of Fig. 5A shows that $L_\alpha$ and $L_\beta$ phases are 4.30 nm and 5.54 nm, respectively, above the mica substrate. As expected, these values and the inter-domain difference are similar to the one seen in Fig. 2 (see Table 2 for comparison). Remarkably, we observed that the close-packed areas of LacY, reside exclusively in the $L_\alpha$ phase (see white arrows). The presence of LacY in the fluid phase was earlier reported to occur in liposomes [29] and follows a general principle for which many membrane proteins are excluded from the gel phase [24,28]. We also demonstrated that photosynthetic complexes are mainly incorporated into the fluid phase, in which they can laterally segregate [17]. In addition, it is thought that highly ordered striated domains of certain peptides are flanked by fluidized lipids [30]. The self-segregation of LacY in fluid phase reflects the difficulties in obtaining, on a plane, well-ordered arrays or 2D crystals of LacY in phospholipid gel phase [6,7]. Thus, the high flexibility attributed to LacY [8–10] results in high lateral mobility in the $L_\alpha$ phase of the bilayer, which favours its segregation and consequent close-packed assembly in such a phase.

Fig. 6A shows a rim formed by two close-packed assemblies of LacY separated by the underlying fluid phospholipid phase. The cross-section analysis in Fig. 6B shows that the close-packed region of proteins is protruding $1.96 \pm 0.18$ nm above the lower phospholipid domains. Hence, it becomes clear that the protein has been inserted into the bilayer. Since, during the reconstitution process, LacY molecules may insert with either the periplasmic or the cytoplasmic loops exposed on the distal layer of the SLB, the height of the protruding areas accounts for the estimated average dimensions of the loops of the protein (Fig. 6C).

In conclusion, we found that LacY can be successfully reconstituted in monomeric form in SPBs of POPE:POPG (3:1, mol/mol). LacY is preferentially inserted in the fluid phospholipid phase, in which it

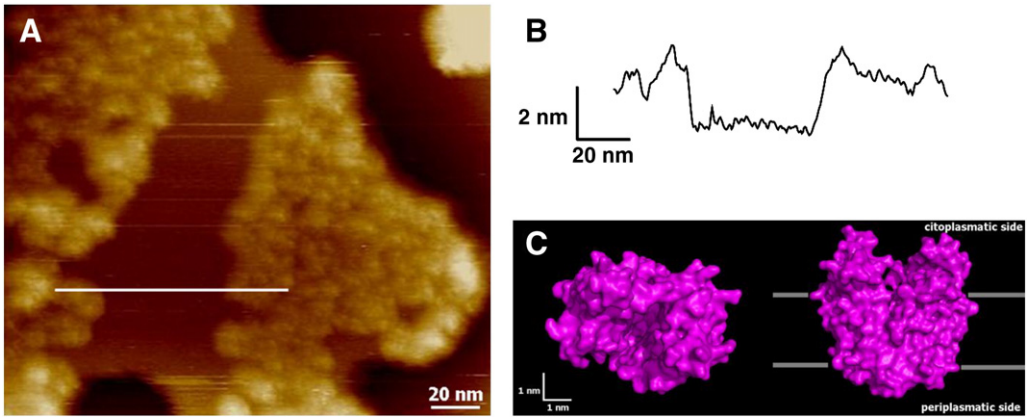


**Fig. 6.** TM-AFM image of a higher magnification of close-packed assemblies of protein found after LacY incorporation in SLB of POPE:POPG (3:1, mol/mol) (A). Line profile analysis along white line is shown in 5B, showing a step-height difference between the protein assemblies and the lipid bilayer in which it is embedded. The diagram showing the frontal cytoplasmic face of the LacY and lateral view showing the region of the protein embedded in the bilayer (C) is taken from Abramson et al. (2003). The *z*-colour scale is 8 nm and the scale bar is 20 nm.

becomes segregated, forming long-range ordering self-segregated protein domains. The diameter of protein monomers compares well with the value obtained from X-ray diffraction data [5]. As the resolution is in nanometer range, we are fairly confident that resolution could be further improved by tuning incorporation and/or imaging conditions.

## Acknowledgements

LP is recipient of a R&D fellowship from the University of Barcelona. This study is supported by Hispano-French bilateral action (HF 2007-0028), the grant CTQ-2008-03922/BQU from the Spanish Government and the ANR PCV program (grant # AFM-MB-PROT).

## References

[1] H.R. Kaback, M. Sahin-Toth, A.B. Weinglass, The kamikaze approach to membrane transport, Nat. Rev. Mol. Cell Biol. 2 (2001) 610–620.
[2] L. Guan, I.N. Smirnova, G. Verner, S. Nagamori, H.R. Kaback, Manipulating phospholipids for crystallization of a membrane transport protein, Proc. Natl. Acad. Sci. USA 103 (2006) 1723–1726.
[3] G.G. Prive, G.E. Verner, C. Weitzman, K.H. Zen, D. Eisenberg, H.R. Kaback, Fusion proteins as tools for crystallization: the lactose permease from Escherichia coli, Acta Crystallogr. D Biol. Crystallogr. 50 (1994) 375–379.
[4] C.K. Engel, L. Chen, G.G. Prive, Insertion of carrier proteins into hydrophilic loops of the Escherichia coli lactose permease, Biochim. Biophys. Acta 1564 (2002) 38–46.
[5] J. Abramson, I. Smirnova, V. Kasho, G. Verner, H.R. Kaback, S. Iwata, Structure and mechanism of the lactose permease of Escherichia coli, Science 301 (2003) 610–615.
[6] J. Zhuang, G.G. Prive, G.E. Werner, P. Ringler, H.R. Kaback, A. Engel, Two-dimensional crystallization of Escherichia coli lactose permease, J. Struct. Biol. 125 (1999) 63–75.
[7] S. Merino-Montero, M.T. Montero, J. Hernández-Borrell, O. Domènech, Preliminary atomic force microscopy study of two-dimensional crystals of lactose permease from Escherichia coli, Biophys. Chem. 119 (2006) 78–83.
[8] J. LeCoutre, L.R. Narasimhan, C.K.N. Patel, H.R. Kaback, The lipid bilayer determines helical tilt angle and function in lactose permease of Escherichia coli, Proc. Natl. Acad. Sci. USA 94 (1997) 10167–10171.
[9] A.B. Weinglass, H.R. Kaback, Conformational flexibility at the substrate binding site in the lactose permease of Escherichia coli, Proc. Natl. Acad. Sci. USA 96 (1999) 11178–11182.
[10] I.N. Smirnova, H.R. Kaback, A mutation in the lactose permease of Escherichia coli that decreases conformational flexibility and increases protein stability, Biochemistry 42 (2003) 3025–3031.
[11] J.L. Rigaud, D. Levy, Reconstitution of membrane proteins into liposomes, Methods Enzymol., Pt B 372 (2003) 65–86.
[12] P. Vitanen, M.J. Newman, D.L. Foster, T.H. Wilson, H.R. Kaback, Purification, reconstitution and characterization of the lac permease of E. coli, Methods in Enzymology 125 (1986) 429.
[13] T.G. Consler, B.L. Persson, H. Jung, K.H. Zen, K. Jung, G.G. Prive, G.E. Verner, H.R. Kaback, Properties and purification of an active biotinylated lactose permease from Escherichia-coli, Proc. Natl. Acad. Sci. USA 90 (1993) 6934–6938.
[14] K. Dornmair, F. Jahnig, Internal dynamics of lactose permease, Proc. Natl. Acad. Sci. USA 86 (1989) 9827–9831.
[15] M. Zhao, K.-. Zen, J. Hernandez-Borrell, H.R. Kaback, C. Altenbach, W.L. Hubbell, Nitroxide scanning electron paramagnetic resonance of helices IV and V and the intervening loop in the lactose permease of Escherichia coli, Biochemistry 38 (1999) 15970–15977.
[16] L. Picas, M.T. Montero, A. Morros, J.L. Vazquez-Ibar, J. Hernandez-Borrell, Evidence of phosphatidylethanolamine and phosphatidylglycerol presence at the annular region of lactose permease of Escherichia coli, Biochim. Biophys. Acta 1798 (2010) 291–296.
[17] P.E. Milhiet, F. Gubellini, A. Berquand, P. Dosset, J.L. Rigaud, C. Le Grimellec, D. Levy, High-resolution AFM of membrane proteins directly incorporated at high density in planar lipid bilayer, Biophys. J. 91 (2006) 3268–3275.
[18] J.L. Vazquez-Ibar, L. Guan, M. Svrakic, H.R. Kaback, Exploiting luminescence spectroscopy to elucidate the interaction between sugar and a tryptophan residue in the lactose permease of Escherichia coli, Proc. Natl. Acad. Sci. USA 100 (2003) 12706–12711.
[19] C. Teichert, Self-organization of nanostructures in semiconductor heteroepitaxy, Physics Reports—Review Section of Physics Letters, vol. 365, 2002, pp. 335–432.
[20] A. Berquand, D. Lévy, F. Gubellini, C. Le Grimellec, P.E. Milhiet, Influence of calcium on direct incorporation of membrane proteins into in-plane lipid bilayer, Ultramicroscopy 107 (2007) 928.
[21] L. Picas, M.T. Montero, A. Morros, M.E. Cabañas, J. Hernández-Borrell, B. Seantier, P.E. Milhiet, Calcium induces domain formation in phosphatidylethanolamine-phosphatidylglycerol bilayers: a combined DSC, $^{31}$P-NMR and AFM study, J. Phys. Chem. B 113 (2009) 4648–4655.
[22] M.C. Giocondi, V. Vie, E. Lesniewska, P.E. Milhiet, M. Zinke-Allmang, C. Le Grimellec, Phase topology and growth of single domains in lipid bilayers, Langmuir 17 (2001) 1653–1659.
[23] F. Kienberger, C. Stroh, G. Kada, R. Moser, W. Baumgartner, V. Pastushenko, C. Rankl, U. Schmidt, H. Muller, E. Orlova, C. LeGrimellec, D. Drenckhahn, D. Blaas, P. Hinterdorfer, Dynamic force microscopy imaging of native membranes, Ultramicroscopy 97 (2003) 229–237.
[24] A.G. Lee, Lipid–protein interactions in biological membranes: a structural perspective, Biochim. Biophys. Acta 1612 (2003) 1–40.
[25] M.O. Jensen, O.G. Mouritsen, Lipids do influence protein function—the hydrophobic matching hypothesis revisited, Biochim. Biophys. Acta 1666 (2004) 205–226.
[26] O. Domenech, J. Ignes-Muollol, M.T. Montero, J. Hernandez-Borrell, Unveiling a complex phase transition in monolayers of a phospholipid from the annular region of transmembrane proteins, J. Phys. Chem. B 111 (2007) 10946–10951.
[27] J.Y. Lehtonen, P.K. Kinnunen, Evidence for phospholipid microdomain formation in liquid crystalline liposomes reconstituted with Escherichia coli lactose permease, Biophys. J. 72 (1997) 1247–1257.
[28] M.D. Houslay, K.K. Stanley, Dynamics of Biological Membranes, influence on synthesis, structure and function, Wiley Interscience, New York, NY, 1982.
[29] L. Thilo, H. Trauble, P. Overath, Mechanistic interpretation of the influence of lipid phase transitions on transport functions, Biochemistry 16 (1977) 1283–1290.
[30] H.A. Rinia, J.W. Boots, D.T. Rijkers, R.A. Kik, M.M. Snel, R.A. Demel, J.A. Killian, J.P. van der Eerden, B. de Kruijff, Domain formation in phosphatidylcholine bilayers containing transmembrane peptides: specific effects of flanking residues, Biochemistry 41 (2002) 2814–2824.